

SEISMIC SOURCE TIME FUNCTION AND FREQUENCY CONTENT OF IMPACT-GENERATED SEISMIC WAVES. N. Wójcicka¹, G. S. Collins¹, I. D. Bastow¹, K. Miljković² and A. Rajšić². ¹Department of Earth Science and Engineering, Imperial College London, London, SW7 2AZ, United Kingdom; ²Space Science and Technology Centre, School of Earth and Planetary Sciences, Curtin University, Perth, Australia; (E-mail: n.wojcicka18@imperial.ac.uk).

Introduction: The InSight mission landed on Mars in late 2018. To date it has recorded a large number of marsquakes [1, 2] but, contrary to pre-landing expectations [3], no impacts. This implies that assumptions used to predict the number of impact detections require revision.

The seismic source function is a crucial element of describing meteorite impacts as seismic sources because it is related to seismic magnitude and can be used as input in wave propagation modelling to predict seismic amplitudes at the receiver location, such as InSight [4]. Frequency spectra produced by meteorite impacts, and their properties, such as peak and cutoff frequency, are likely to be related to both impactor and target properties [5–7]. Characterising the frequency spectra will help explore whether impacts on Mars in fact generate signals with different frequency content to that previously assumed when InSight forecasts were made.

We forward model the impact process to constrain the seismic signature of meteorite impacts in terms of their equivalent seismic force function and frequency content.

Theory:

Source function The time integral of the seismic force function, $\mathbf{F}(t)$, gives the seismic impulse produced, \mathbf{I} , which is by definition equal to the momentum transferred to the target by the impact, $\mathbf{p}(t)$ [8]. Because we consider strictly vertical impact scenarios, we assume that the equivalent seismic source is a vertical force, $F_z(t)$, which depends on the vertical momentum transferred, $p_z(t)$. Hence:

$$I = \int_0^\tau F_z(t) dt = p_z(t), \quad (1)$$

where τ is the source duration. We can compute the seismic force as a function of time by differentiating the momentum transferred during impact:

$$F_z(t) = \frac{d(p_z(t))}{dt}. \quad (2)$$

Frequency content The frequency content of impact-generated seismic waves has not been well constrained in the past, although previous studies analysing impacts on the Moon [5, 6] suggested that meteorite impacts exhibit a low cutoff frequency and depends heavily on the geology of the impact site. On the other hand, [7] found that impact clusters show a higher cutoff frequency than singular impact events.

A recently published study [9] used a Lagrangian hy-

drocode to determine the frequency spectrum of elastic waves produced by impact onto a rocky asteroid. Here we adopt the same approach to determine the frequency spectrum of impact-generated seismic waves into targets with a range of material properties, from hard dense rock to soft, porous regolith. We start by reproducing one of the numerical experiments of [9] using the Eulerian version of iSALE2D. We then extend this work to Martian conditions and investigate the sensitivity of the frequency content to target properties and impact momentum.

Modelling: All simulations in this work were carried out using iSALE2D [10–12].

Source function We simulated a 4.4-cm impactor striking a Mars-like regolith at 1.93 km/s. The impactor is represented as a sphere of non-porous basalt of density $\rho = 2860 \text{ kgm}^{-3}$, using a Tillotson equation of state [13] and Lundborg strength model [14]. The target is modelled as a 44% porous basalt of density $\rho = 1589 \text{ kgm}^{-3}$, using a Tillotson equation of state and Lundborg strength model (see [15]). The simulation domain comprised 1500 cells in the radial and vertical directions with an impactor resolution of 10 cells per projectile radius (cpr). The simulation ran for 1 ms, at a high temporal resolution of 5×10^{-6} s, needed to resolve the very sharp initial rise in the source function. We calculate the momentum transferred to the target using equation (13) of [15]:

$$p_z = \int_V \rho v_z dV, \quad (3)$$

where ρ is the target density, v_z is material velocity and V is the source volume. This is evaluated at every save time of the simulation and the resulting time series is integrated using equation (2), to produce force as a function of time (Fig.1).

Frequency content We reproduce the numerical experiments from [9] that simulate a 60-m impactor striking the surface of a 1 km wide asteroid at 100 m/s. The target and impactor are each modelled as a non-porous basaltic sphere of density $\rho = 2860 \text{ kgm}^{-3}$, using a Tillotson equation of state and Lundborg strength model. The simulation domain consists of 500 cells vertically and 250 cells horizontally, with the impactor resolution of 15 cpr. A low impact speed and a very high target cohesion of 100 MPa, are used to ensure a near-elastic response of the target. We use a Lagrangian probe placed 2 m under the asteroid's surface at its equator, to record the displacement at high temporal resolution. A Fast Fourier Transform is then ap-

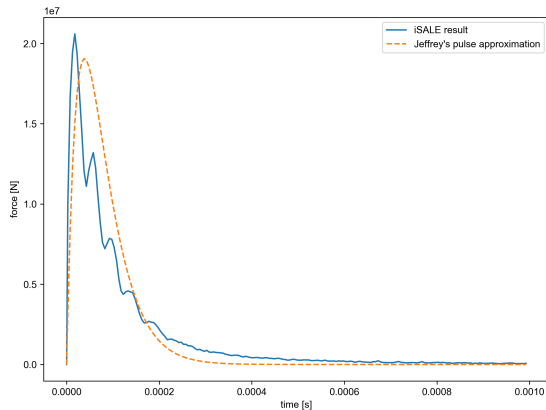


Figure 1: Source-time function calculated for a simulation of 1-kg impactor striking the Martian surface at 1.93 km/s (blue solid line) and a best fit Jeffrey's pulse (dashed line).

plied to the seismogram to produce a frequency spectrum.

Results & Discussion:

Source function Our simulation produces a force function with a sharp initial rise in the first 0.01 ms after impact, and a peak force reached $F_{max} = 2.1 \times 10^7$ N. The duration of the source, τ , for this model was ~ 0.5 ms (Fig.1). The oscillations observed as the force decays are attributed to the shock wave travelling through the impactor and back down to the target.

The source function can be approximated using an integrable model function such as a Jeffrey's pulse:

$$F_J = \alpha^2 p_i t e^{-\alpha t}, \quad (4)$$

where α is a time constant that governs the duration and peak amplitude of the source. We use a least-squares approach to estimate the value of $\alpha = 2.6 \times 10^4 \text{ s}^{-1}$. The best-fit approximation slightly underestimates both the source duration ($\tau \approx 3 \times 10^{-4} \text{ s}$) and the peak force reached ($F_{max} = 1.9 \times 10^7 \text{ N}$). Integrating F_J recovers numerical value of p_z to within 4 %.

Frequency content Fig. 2 shows a frequency spectrum for the simulation of a 60-m impactor striking an asteroid. The peak frequency at about 10 Hz is consistent with the results of [9]. Our simulations show less energy at frequencies lower than 10 Hz, which could reflect the use of higher target density and lower cohesion in our material model compared to the original study. We aim to extend this work to examine the effect of impact velocity and target material properties on the frequency spectrum.

Conclusions: We calculate the equivalent seismic source function for a nominal impact scenario. We characterise the resulting function in terms of source duration ($\tau \approx 5 \times 10^{-4} \text{ s}$) and peak force released ($F_{max} = 2.1 \times 10^7 \text{ N}$).

We have tested a method for obtaining a frequency

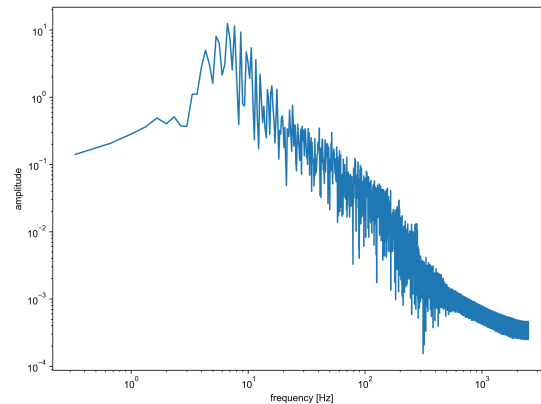


Figure 2: Vertical frequency spectrum for a 60-m impactor striking a 1-km wide asteroid at 100 m/s, recorded 2 m under the surface at the equator of the asteroid.

spectrum from a hydrocode simulation of a meteorite impact onto a rocky asteroid. We will eventually extend this work to investigate the influence of impact properties (impactor momentum and target material properties) on both the frequency spectrum and source time function.

This work will aid understanding of impact-generated seismic waves and help distinguish them from waves generated by tectonic sources. It will also help understand the lack of impact detections at InSight to date.

Acknowledgements: We gratefully acknowledge the developers of iSALE (www.isale-code.de) and the UK Space Agency for funding (Grants ST/S001514/1 and ST/T002026/1). KM is fully funded by the Australian Research Council (DE180100584, DP180100661).

References: [1] Giardini, D. et al. (2020) *Nat. Geosci.* in press. [2] Banerdt, W. B. et al. (2020) *Nat. Geosci.* 13:183–189. [3] Daubar, I. J. et al. (2020) *J. Geophys. Res. Planets*, [4] Daubar, I. J. et al. (2018) *Space Sci. Rev.* 214:132. [5] Gudkova, T. et al. (2011) *Icarus*, 211:1049–1065. [6] Gudkova, T. et al. (2015) *Earth Planet. Sci. Lett.* 427:57–65. [7] Schmerr, N. C. et al. (2019) *J. Geophys. Res. Planets*, 124:3063–3081. [8] Lognonné, P. et al. (2009) *J. Geophys. Res.* 114:E12003. [9] Richardson, J. E. et al. (2020) *Icarus*, 347:113811. [10] Amsden, A. A. et al. (1980) tech. rep. June Los Alamos, NM (United States): Los Alamos National Laboratory (LANL), 101p. [11] Collins, G. S. et al. (2004) *Meteorit. Planet. Sci.* 39:217–231. [12] Wünnemann, K. et al. (2006) *Icarus*, 180:514–527. [13] Tillotson, J. H. (1962) *Rep. No. GA-3216, Gen. At. San Diego, CA*, 43. [14] Lundborg, N. (1968) *Int. J. Rock Mech. Min. Sci.* 5:427–454. [15] Wójcicka, N. et al. (2020) *J. Geophys. Res. Planets*, 125.